JOURNAL OF MECHANICAL ENGINEERING AND SCIENCES (JMES)
ISSN: 2289-4659 e-ISSN: 2231-8380
VOL. 14, ISSUE 3, 7205 – 7221
DOI: https://doi.org/10.15282/jmes.14.3.2020.21.0566

ORIGINAL ARTICLE

A comparative study on the vibration of functionally graded Magneto-Electro-Elastic rectangular plate rested on a Pasternak foundation based on exponential and first-order shear deformation theories

H.R. Talebi Amanieh[1], S.A. Seyed Roknizadeh[1,2], A. Reza[1]

[1] Department of Mechanical Engineering, Ahvaz Branch, Islamic Azad University, Ahvaz, Iran
Phone: +986133348420-4; Fax: +986133329200
[2] Department of Mechanical Engineering, Faculty of Engineering, Shahid Chamran University of Ahvaz, Ahvaz, Iran

ABSTRACT – In this paper, the in-plane and out-of-plane free vibrations of the functionally graded magneto-electro-elastic (FG-MEE) rectangular plate on a pasternak foundation were evaluated based on exponential shear deformation theory (ESDT) and first order shear deformation theory (FSDT). The material properties of FG-MEE varied along the thickness according to a power-law distribution model. It was assumed that the FG-MEE plate is subjected to initial external electrical and magnetic potentials; mreover, simply-supported boundary conditions were considered for all the edges of the FG-MEE plate. Firstly, the corresponding partial differential equations (PDEs) were derived using Hamilton's principle, then, the natural frequencies were determined by solving the obtained equations through Navier's approach according to the assumed boundary conditions. The results revealed that the natural frequencies of the plate decrease/increase with the increase of the electric/magnetic potentials. Moreover, the results showed a 0.03%, difference between the natural frequencies of the plate with a thickness-to-length ratio of 0.1 based on FSDT and ESDT; when the aspect ratio was increased to 0.2 and 0.3 this difference rose to 0.2% and 0.5%, respectively.

ARTICLE HISTORY
Revised: 28th Apr 2020
Accepted: 15th May 2020

KEYWORDS
FG-MEE plate; in-plane vibrations; out-of-plane vibrations; first-order shear deformation theory; exponential shear deformation theory; Pasternak foundation

INTRODUCTION

The exprimental and theorical dynamic responses of elastic bodies and applications under various external conditions have been investigated by many researchers [1-8] . Furthermore, the vibration analysis of a thin plate, with or without piezoelectric effects, has been the subject of several investigations. The electrostatic coupling effect of piezoelectric structures is defined as their ability to transform mechanical strains into electrical signals or vice versa. This effect has been also examined extensively over the past decades [9-12]. Regarding the substantial application of transverse vibrations in rectangular plates, several investigations have been devoted to this subject [13]. However, despite the probability of exciting in-plane vibrations in some structures, only a few studies have been focused on in-plane free vibrations due to the higher values of in-plane natural frequencies compared to the excitation frequencies.

Bardell et al. [14] studied the free vibrations of isotropic rectangular plates using the Rayleigh-Ritz method for simply-supported, clamped, and free boundary conditions. Farag and Pan [15] investigated the free and forced in-plane vibrations of rectangular plates; however, the forced responses were only studied in excitation with in-plane point force using orthogonal properties of the mode shapes and modal characteristics in different boundary conditions. The closed-form solutions were addressed for the in-plane vibrations of rectangular plates with simply-supported and clamped boundary conditions by Gorman [16-18] through superposition methods. In another study by Hosseini Hashemi and Moradi, a closed-form solution was obtained for the Mindlin plate using the Helmholtz decomposition [19]. Xing and Liu [20] presented exact solutions for in-plane free vibration of rectangular plates using the direct separation method. In-plane natural frequencies and mode shapes of composite materials were examined by Dozio and Lorenzo [21] through the use of the Ritz method.

Recent years have witnessed remarkable developments in the field of intelligent materials, including piezoelectric and piezomagnetic materials. These materials are capable of converting one form of energy (e.g. magnetic, electrical, and mechanical) to another; they re also called magneto-electro-elastic (MEE) composites.

Pan and Heyliger [22] investigated the linear vibrations of multilayer MEE rectangular plates under simply-supported boundary conditions using the theory of thin plates and classical plate theory. They also derived the governing equations, natural frequencies, and mode shape by propagator matrix method. Buchanan and George [23] examined and compared the vibrations of the multi-layered and multi-phase MEE plates. They obtained a solution by extracting shape functions using Galerkin's finite element method and considering the 3-node elements.

In 2010, Liu et al. [24] studied the exact solution for the vibrations of isotropic MEE rectangular thin plates. They looked for an exact free vibration solution for two-layered material consisting of $BaTiO_3$-$CoFe_2O_4$; besides, the effect of volume fraction on natural frequencies was addressed. In 2014, free vibrations of MEE plates on elastic foundation were

*CORRESPONDING AUTHOR | S.A. Seyed Roknizadeh | ✉ s.roknizadeh@scu.ac.ir

investigated by Li and Zhang [25] using first-order shear deformation theory (also known as Mindlin theory). Ke et al. [26] analyzed the free vibration of MEE nanoplates based on classical and nonlocal theories.

Recently, a new class of advanced materials has been introduced in the field of intelligent structures known as functionally grade Magneto-electro-elastic (FG-MEE) products. These materials can be exploited in sensors and actuators. Unlike ordinary multi-layered plates with abrupt material properties variations between the layers, these plates are benefited from the gradual alteration of material properties across their thickness which can significantly improve their performance and life.

In 2005, Bhangale and Ganesan [27] investigated the free vibrations of nonhomogeneous FG-MEE cylindrical shells under simply-supported boundary conditions. The inner and outer surfaces of the shell were made from piezoelectric and piezomagnetic materials, respectively, and the problem was solved by the use of the finite element method introduced by Buchanan [28]. Tsai and Wu [29] in 2008 used an approximated method to evaluate the three-dimensional (3-D) free vibration of FG-MEE shells with simply-supported boundary conditions and solved the derived equations using the state space method. Wu and Lu [30] analyzed the vibrations of FG-MEE rectangular plates by modified Pagano's method considering a 3-D plate under simply-supported boundary conditions. The multi-scale method was utilized for solving the 3-D vibrations of FG-MEE shells under simply-supported boundary conditions and classical shell theory assumptions by Wu and Tsai[31] . Hosseini et al.[32] evaluated the sensitivity of FG-MEE nanoplates with attached nanoparticles as a nanosensor considering nonlocal Mindlin plate assumption and using the Navier's method. Shooshtari and Mantashloo [33] studied the linear and nonlinear free vibrations of the FG-MEE rectangular plates based on third-order shear deformation theory. By omitting the rotational and in-plane inertia terms, they obtained the vibrational equations and solved the equations using Lindstedt- Poincare method.

Exponential shear deformation theory was first proposed by Karama et al. [34] in 2003 during studying a multilayer beam. Their new multi-layered structure exponential model exactly and automatically satisfied the continuity condition of displacements and transverse shear stresses at interfaces, as well as the boundary conditions for a laminated composite with the help of the Heaviside step function. Sayyed and Ghugal [35] examined the buckling and free vibrations of isotropic thick plates with exponential shear deformation theory. In their research, the exponential functions were aligned to the applied thickness and the displacements included shear transverse deformation and rotational inertia. The frequencies obtained by the ESDT theory for all modes of vibration were in excellent agreement with the exact values and higher-order shear deformation theory of frequencies for the simply supported square plate. Kharde et al. [36] investigated the isotropic plate vibrations using exponential shear deformation theory. They obtained the differential equations and boundary conditions using the principle of virtual work and their results were compared with the results of other shear deformation theories as well as the exact solutions found in other papers. Khorshidi et al. [37, 38] investigated the free vibration and buckling of rectangular nano-plates based on a nonlocal theory with exponential shear deformation. Khorshidi et al. [39] investigated the free vibrations of functionally graded composite rectangular nanoplates based on the nonlocal theory by exponential shear deformation in the thermal environment.

First-order shear deformation theory (FSDT) can be considered as an improvement to the classical plate theory (CPT). It is based on the hypothesis that the normal to the undeformed mid-plane remains straight but not necessarily normal to the mid-plane after deformation. This is known as FSDT because the thickness-wise displacement field for the in-plane displacement is linear or of the first order. In Mindlin's theory, the transverse shear stress is assumed to be constant through the thickness of the plate, but this assumption violates the shear stress-free surface conditions on the top and bottom of the plate. Exponential shear deformation theory (ESDT) is used for free vibration analysis of thick rectangular plates which includes the effect of transverse shear deformation and rotary inertia. The displacement field of the theory contains three variables as in the FSDT of the plate.

The FG-MEE materials are a new class of smart materials with coupling electrical, magnetic, and mechanical properties whose exact behavior has to be properly explored. In fact, to improve our understanding of these materials it is necessary to analyze them with higher-order theories such as ESDT and examine the validity of more common theories such as FSDT. To the best of the authors' knowledge, there is no available literature in the field of in-plane and out-of-plane vibrations of FG-MEE plates on Pasternak foundation based on the exponential shear deformation theory and first-order shear deformation theory. Accordingly, in this paper, the equations of plate displacement were written based on the ESDT and FSDT and the constitutive equations were obtained. Moreover, the electrical and magnetic potential functions were obtained according to the initial conditions which satisfied the Maxwell equations as well. Finally, Navier's method was used to solve the differential equations obtained based on the Hamilton principle.

KINEMATICS OF DIFFERENT THEORIES

A moderately thick FG-MEE rectangular plate with the respective length, width, and thickness of a, b, and h with simply-supported edges was considered in this research as depicted in Figure 1.

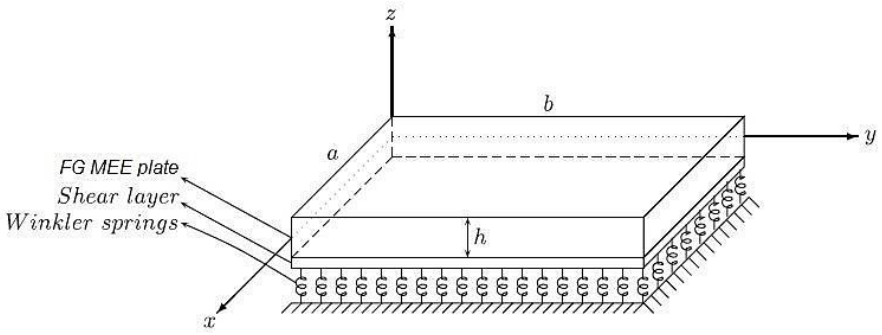

Figure 1. FG-MEE Rectangular plate rest on Pasternak foundation

According to Figure 2, the considered FG plate is constructed from piezomagnetic ($CoFe_2O_4$) and piezoelectric ($BaTiO_3$) materials. It is assumed that the material properties continuously varied across the plate thickness according to the power-law model as follows [30]:

$$P(z) = (P_2 - P_1)(\frac{z}{h} + \frac{1}{2})^p + P_1 \tag{1}$$

where, P represents the properties of the constructed materials, including Young's modulus, density, and electrical and magnetic coefficients. In this research, P_1 and P_2 correspond to the properties of $CoFe_2O_4$ and $BaTiO_3$, respectively.

Figure 2. FG-MEE Rectangular plate

Exponential Shear Deformation Theory

The displacement fields can be expressed according to the exponential shear deformation theory as follows [38]:

$$\begin{aligned} u(x,y,z,t) &= u_0(x,y,t) - z\frac{\partial w(x,y,t)}{\partial x} + f(z)\theta_x(x,y,t) \\ v(x,y,z,t) &= v_0(x,y,t) - z\frac{\partial w(x,y,t)}{\partial y} + f(z)\theta_y(x,y,t) \\ w(x,y,z,t) &= w(x,y,t) \end{aligned} \tag{2}$$

where $f(z) = z\left(e^{-2\left(\frac{z}{h}\right)^2}\right)$. u_0, v_0 and w_0 are the mid-plane displacements in x, y, and z directions, respectively. θ_x and θ_y denote the rotations of the mid-plane along the x and y axes, respectively.

Based on the above relations for displacement, linear strains for a rectangular plate can be expressed as follows [36]:

$$\begin{aligned} \varepsilon_x &= u_{,x} = u_{0,x} - z\,w_{,xx} + f(z)\theta_{x,x} \\ \varepsilon_y &= v_{,y} = v_{0,y} - z\,w_{,yy} + f(z)\theta_{y,y} \\ \gamma_{xz} &= u_{,z} + w_{,x} = f(z)_{,z}\theta_x \\ \gamma_{yz} &= v_{,z} + w_{,y} = f(z)_{,z}\theta_y \\ \gamma_{xy} &= u_{,y} + v_{,x} = u_{0,y} + v_{0,x} - 2z\,w_{,xy} + f(z)(\theta_{x,y} + \theta_{y,x}) \end{aligned} \tag{3}$$

First-order Shear Deformation Theory

The displacement fields can be expressed according to the first-order shear deformation theory as follows [30]:

$$\begin{aligned} u(x,y,z,t) &= u_0(x,y,t) + z\theta_x(x,y,t) \\ v(x,y,z,t) &= v_0(x,y,t) + z\theta_y(x,y,t) \end{aligned} \tag{4}$$

where u_0, v_0 and w_0 are the mid-plane displacements in x, y, and z directions, respectively. θ_x and θ_y denote the rotations of the mid-plane along the x and y axes, respectively.

Based on the above relations for displacement, linear strains for a rectangular plate can be expressed as [30]:

$$\begin{aligned}
\varepsilon_x &= u_{,x} = u_{0,x} + z\theta_{x,x} \\
\varepsilon_y &= v_{,y} = v_{0,y} + z\theta_{y,x} \\
\gamma_{xz} &= u_{,z} + w_{,x} = k(w_{0,x} + \theta_x) \\
\gamma_{yz} &= v_{,z} + w_{,y} = k(w_{0,y} + \theta_y) \\
\gamma_{xy} &= u_{,y} + v_{,x} = u_{0,y} + v_{0,x} + z(\theta_{x,y} + \theta_{y,x})
\end{aligned} \tag{5}$$

CONSTITUTIVE EQUATION

The constitutive equations of FG-MEE are given in the following form [30]:

$$\begin{aligned}
\sigma &= C(z)\varepsilon - e(z)E - q(z)H \\
D &= e(z)^T\varepsilon + \eta(z)E + d(z)H \\
B &= q(z)^T\varepsilon + d(z)E + \mu(z)H
\end{aligned} \tag{6}$$

where, σ, ε, D, B, E and H are stress vector, strain vector, electrical displacement, magnetic flux vector, electric field, and magnetic field vectors, respectively. C, η, μ, e, q, and d are matrices corresponding to the elastic, dielectric, magnetic, piezoelectric piezomagnetic, and magneto-electric coefficients, respectively. As mentioned before, these coefficients are not constant along the thickness of FG-MEE materials and vary as a function of z according to Eq. (1).

The matrix representation of the above-mentioned coefficients can be written as:

$$C(z) = \begin{bmatrix} c_{11}(z) & c_{12}(z) & 0 & 0 & 0 \\ c_{12}(z) & c_{22}(z) & 0 & 0 & 0 \\ 0 & 0 & c_{44}(z) & 0 & 0 \\ 0 & 0 & 0 & c_{55}(z) & 0 \\ 0 & 0 & 0 & 0 & c_{66}(z) \end{bmatrix} \quad \mu(z) = \begin{bmatrix} \mu_{11}(z) & 0 & 0 \\ 0 & \mu_{22}(z) & 0 \\ 0 & 0 & \mu_{33}(z) \end{bmatrix}$$

$$e(z) = \begin{bmatrix} 0 & 0 & e_{31}(z) \\ 0 & 0 & e_{32}(z) \\ 0 & e_{24}(z) & 0 \\ e_{15}(z) & 0 & 0 \\ 0 & 0 & 0 \end{bmatrix} \quad q(z) = \begin{bmatrix} 0 & 0 & q_{31}(z) \\ 0 & 0 & q_{32}(z) \\ 0 & q_{24}(z) & 0 \\ q_{15}(z) & 0 & 0 \\ 0 & 0 & 0 \end{bmatrix} \tag{7}$$

$$\eta(z) = \begin{bmatrix} \eta_{11}(z) & 0 & 0 \\ 0 & \eta_{22}(z) & 0 \\ 0 & 0 & \eta_{33}(z) \end{bmatrix} \quad d(z) = \begin{bmatrix} d_{11}(z) & 0 & 0 \\ 0 & d_{22}(z) & 0 \\ 0 & 0 & d_{33}(z) \end{bmatrix}$$

It should be noted that if the electric and magnetic fields are a negative scalar gradient of electrical and magnetic potentials, the Maxwell Equations can be written considering quasi-static approximation [30]:

$$\begin{aligned}
E_j &= -\frac{\partial \Phi(x,y,z,t)}{\partial j} \\
H_j &= -\frac{\partial \Psi(x,y,z,t)}{\partial j} \qquad (j = x,y,z)
\end{aligned} \tag{8}$$

It is supposed that the MEE plate is subjected to the electrical potential of $\phi_0$and magnetic potential of ψ_0 boundary conditions in the upper and lower surfaces of the plate along the z direction. These boundary conditions are expressed as follows:

$$\begin{aligned}
&\Phi\left(x,y,-\frac{h}{2},t\right) = -\phi_0 \ , \ \Phi\left(x,y,\frac{h}{2},t\right) = \phi_0 \\
&\Psi(x,y,-\frac{h}{2},t) = -\psi_0 \ , \ \Psi(x,y,\frac{h}{2},t) = \psi_0
\end{aligned} \tag{9}$$

Regarding the mentioned electromagnetic boundary conditions, the distributions of electrical and magnetic potentials can be expressed as a sum of the cosine function and linear variations [30]:

$$\begin{aligned}
\Phi(x,y,z,t) &= -\cos\left(\frac{\pi z}{h}\right)\phi(x,y,t) + \frac{2z\phi_0}{h} \\
\Psi(x,y,z,t) &= -\cos\left(\frac{\pi z}{h}\right)\psi(x,y,t) + \frac{2z\psi_0}{h}
\end{aligned} \tag{10}$$

EQUATION OF MOTION

The governing differential equations of motion for an FG-MEE rectangular plate can be derived using Hamilton's principle:

$$\int_{t_1}^{t_2}(\delta T-\delta U+\delta V)=0 \tag{11}$$

where $\delta T, \delta U$, and δV denote the virtual kinetic energy, the virtual strain energy, and the virtual work done by externally applied forces, respectively. To obtain the kinetic and potential energies for the studied plate, the following equations can be used:

$$\begin{aligned} U &= \frac{1}{2}\iiint_v(\sigma_x\varepsilon_x+\sigma_x\varepsilon_x+\tau_{xy}\gamma_{xy}+\tau_{yz}\gamma_{yz}+\tau_{xz}\gamma_{xz})dV \\ T &= \frac{1}{2}\iint_s \rho(z)(\dot{u}^2+\dot{v}^2+\dot{w}^2)dS \end{aligned} \tag{12}$$

$$\delta T=\int\begin{bmatrix} I_0(\dot{u}_0\delta\dot{u}_0+\dot{v}_0\delta\dot{v}_0+\dot{w}_0\delta\dot{w}_0) \\ +I_1(\dot{u}_0\delta\dot{\theta}_x+\dot{\theta}_x\delta\dot{u}_0+\dot{v}_0\delta\dot{\theta}_y+\dot{\theta}_y\delta\dot{v}_0) \\ +I_2(\dot{\theta}_x\delta\dot{\theta}_x+\dot{\theta}_y\delta\dot{\theta}_y)\end{bmatrix}dA$$

$$\begin{aligned} \delta U=&\int\begin{bmatrix} N_x\frac{\partial\delta u_0}{\partial x}+N_y\frac{\partial\delta v_0}{\partial y}+M_x\frac{\partial\delta\theta_x}{\partial x}+M_y\frac{\partial\delta\theta_y}{\partial y} \\ +N_{xy}(\frac{\partial\delta u_0}{\partial y}+\frac{\partial\delta v_0}{\partial x})+M_{xy}(\frac{\partial\delta\theta_x}{\partial y}+\frac{\partial\delta\theta_y}{\partial x}) \\ +Q_x(\delta\theta_x+\frac{\partial\delta w_0}{\partial x})+Qy(\delta\theta_y+\frac{\partial\delta w_0}{\partial y})\end{bmatrix}dA \\ &-\int\int_{-\frac{h}{2}}^{\frac{h}{2}}\begin{pmatrix} D_x\delta E_x+D_y\delta E_y+D_z\delta E_z \\ +B_x\delta H_x+B_y\delta H_y+B_z\delta H_z\end{pmatrix}dzdA \end{aligned} \tag{13}$$

$$\delta V=\int q\delta w_0 dA$$

$$q=-k_w w_0+k_s(w_{0,xx}+w_{0,yy})+(N_{Ex}+N_{Mx})w_{0,xx}+(N_{Ey}+N_{My})w_{0,yy}$$

ESDT

According to Eq. (13), forces and momentums are defined as follows:

$$\begin{aligned} \begin{Bmatrix}N_x\\N_y\\N_{xy}\end{Bmatrix}&=\int_{\frac{h}{2}}^{-\frac{h}{2}}\begin{Bmatrix}\sigma_x\\\sigma_y\\\tau_{xy}\end{Bmatrix}dz \qquad \begin{Bmatrix}M_x\\M_y\\M_{xy}\end{Bmatrix}=\int_{\frac{h}{2}}^{-\frac{h}{2}}\begin{Bmatrix}\sigma_x\\\sigma_y\\\tau_{xy}\end{Bmatrix}zdz \\ \begin{Bmatrix}R_x\\R_y\\R_{xy}\end{Bmatrix}&=\int_{h/2}^{-h/2}\begin{Bmatrix}\sigma_x\\\sigma_y\\\tau_{xy}\end{Bmatrix}f(z)\ dz \quad \begin{Bmatrix}Q_x\\Q_y\end{Bmatrix}=\int_{\frac{h}{2}}^{-\frac{h}{2}}\begin{Bmatrix}\tau_{xz}\\\tau_{yz}\end{Bmatrix}f(z)_{,z}\ dz \\ \begin{Bmatrix}I_0\\I_1\\I_2\end{Bmatrix}&=\int_{\frac{h}{2}}^{-\frac{h}{2}}\begin{Bmatrix}1\\z\\z^2\end{Bmatrix}\rho(z)dz \qquad \begin{Bmatrix}I_3\\I_4\\I_5\end{Bmatrix}=\int_{h/2}^{-h/2}\begin{Bmatrix}f(z)\\z\,f(z)\\f(z)^2\end{Bmatrix}\rho(z)\ dz \end{aligned} \tag{14}$$

The governing equations of motion for the rectangular plate are expressed as follows:

$$
\begin{aligned}
&N_{x,x} + N_{xy,y} = I_0\ddot{u} - I_1\ddot{w}_{,x} + I_3\ddot{\theta}_x \\
&N_{y,y} + N_{xy,x} = I_0\ddot{v} - I_1\ddot{w}_{,y} + I_3\ddot{\theta}_y \\
&R_{x,x} + R_{xy,y} - Q_x = I_3\ddot{u} - I_4\ddot{w}_{,x} + I_5\ddot{\theta}_x \\
&R_{y,y} + R_{xy,x} - Q_y = I_3\ddot{v} - I_4\ddot{w}_{,y} + I_5\ddot{\theta}_y \\
&M_{x,xx} + 2M_{xy,xy} + M_{y,yy} + q = I_0\ddot{w} + I_1(\ddot{u}_{,x} + \ddot{v}_{,y}) - I_2(\ddot{w}_{,xx} + \ddot{w}_{,yy}) + I_4(\ddot{\theta}_{x,x} + \ddot{\theta}_{y,y}) \\
&\int_{z_k}^{z_{k+1}} \left(\frac{\partial D_x}{\partial x}\mathrm{Cos}(\frac{\pi z}{h}) + \frac{\partial D_y}{\partial y}\mathrm{Cos}(\frac{\pi z}{h}) + \frac{\pi}{h} D_z \mathrm{Sin}(\frac{\pi z}{h}) \right) dz = 0 \\
&\int_{z_k}^{z_{k+1}} \left(\frac{\partial B_x}{\partial x}\mathrm{Cos}(\frac{\pi z}{h}) + \frac{\partial B_y}{\partial y}\mathrm{Cos}(\frac{\pi z}{h}) + \frac{\pi}{h} B_z \mathrm{Sin}(\frac{\pi z}{h}) \right) dz = 0
\end{aligned}
\tag{15}
$$

By substituting the displacement from Eq. (2) into the strain of Eq. (3) and rewriting Eq. (14), we will have:

$$
\begin{Bmatrix} N_x \\ N_y \\ N_{xy} \end{Bmatrix} = \int_{z_k}^{z_{k+1}} \begin{bmatrix} c_{11}(z) & c_{12}(z) & 0 \\ c_{12}(z) & c_{22}(z) & 0 \\ 0 & 0 & c_{66}(z) \end{bmatrix} \begin{Bmatrix} u_{0,x} - z\, w_{,xx} + f(z)\theta_{x,x} \\ v_{0,y} - z\, w_{,yy} + f(z)\theta_{y,y} \\ u_{0,y} + v_{0,x} - 2z\, w_{,xy} + f(z)(\theta_{x,y} + \theta_{y,x}) \end{Bmatrix} dz
$$

$$
- \int_{z_k}^{z_{k+1}} \begin{bmatrix} 0 & 0 & e_{31}(z) \\ 0 & 0 & e_{32}(z) \\ 0 & 0 & 0 \end{bmatrix} \begin{Bmatrix} 0 \\ 0 \\ -\phi_{,z} \end{Bmatrix} dz - \int_{z_k}^{z_{k+1}} \begin{bmatrix} 0 & 0 & q_{31}(z) \\ 0 & 0 & q_{32}(z) \\ 0 & 0 & 0 \end{bmatrix} \begin{Bmatrix} 0 \\ 0 \\ -\psi_{,z} \end{Bmatrix} dz
$$

$$
\begin{Bmatrix} R_x \\ R_y \\ R_{xy} \end{Bmatrix} = \int_{z_k}^{z_{k+1}} \begin{bmatrix} c_{11}(z) & c_{12}(z) & 0 \\ c_{12}(z) & c_{22}(z) & 0 \\ 0 & 0 & c_{66}(z) \end{bmatrix} \begin{Bmatrix} u_{0,x} - z\, w_{,xx} + f(z)\theta_{x,x} \\ v_{0,y} - z\, w_{,yy} + f(z)\theta_{y,y} \\ u_{0,y} + v_{0,x} - 2z\, w_{,xy} + f(z)(\theta_{x,y} + \theta_{y,x}) \end{Bmatrix} f(z)\ dz
$$

$$
- \int_{z_k}^{z_{k+1}} \begin{bmatrix} 0 & 0 & e_{31}(z) \\ 0 & 0 & e_{32}(z) \\ 0 & 0 & 0 \end{bmatrix} \begin{Bmatrix} 0 \\ 0 \\ -\phi_{,z} \end{Bmatrix} f(z)\, dz - \int_{z_k}^{z_{k+1}} \begin{bmatrix} 0 & 0 & q_{31}(z) \\ 0 & 0 & q_{32}(z) \\ 0 & 0 & 0 \end{bmatrix} \begin{Bmatrix} 0 \\ 0 \\ -\psi_{,z} \end{Bmatrix} f(z)\ dz
$$

$$
\begin{Bmatrix} Q_y \\ Q_x \end{Bmatrix} = \int_{z_k}^{z_{k+1}} \begin{bmatrix} c_{44}(z) & 0 \\ 0 & c_{55}(z) \end{bmatrix} \begin{Bmatrix} f(z)_{,z}\theta_y \\ f(z)_{,z}\theta_x \end{Bmatrix} f(z)_{,z} dz
$$

$$
- \int_{z_k}^{z_{k+1}} \begin{bmatrix} e_{24}(z) & 0 \\ 0 & e_{15}(z) \end{bmatrix} \begin{Bmatrix} E_y \\ E_x \end{Bmatrix} f(z)_{,z} dz - \int_{z_k}^{z_{k+1}} \begin{bmatrix} q_{24}(z) & 0 \\ 0 & q_{15}(z) \end{bmatrix} \begin{Bmatrix} H_y \\ H_x \end{Bmatrix} f(z)_{,z}\, dz
$$

$$
\begin{Bmatrix} M_x \\ M_y \\ M_{xy} \end{Bmatrix} = \int_{z_k}^{z_{k+1}} \begin{bmatrix} c_{11}(z) & c_{12}(z) & 0 \\ c_{12}(z) & c_{22}(z) & 0 \\ 0 & 0 & c_{66}(z) \end{bmatrix} \begin{Bmatrix} u_{0,x} - z\, w_{,xx} + f(z)\theta_{x,x} \\ v_{0,y} - z\, w_{,yy} + f(z)\theta_{y,y} \\ u_{0,y} + v_{0,x} - 2z\, w_{,xy} + f(z)(\theta_{x,y} + \theta_{y,x}) \end{Bmatrix} z dz
$$

$$
- \int_{z_k}^{z_{k+1}} \begin{bmatrix} 0 & 0 & e_{31}(z) \\ 0 & 0 & e_{32}(z) \\ 0 & 0 & 0 \end{bmatrix} \begin{Bmatrix} 0 \\ 0 \\ -\phi_{,z} \end{Bmatrix} z dz - \int_{z_k}^{z_{k+1}} \begin{bmatrix} 0 & 0 & q_{31}(z) \\ 0 & 0 & q_{32}(z) \\ 0 & 0 & 0 \end{bmatrix} \begin{Bmatrix} 0 \\ 0 \\ -\psi_{,z} \end{Bmatrix} z dz \tag{16}
$$

$$
\begin{Bmatrix} D_x \\ D_y \\ D_z \end{Bmatrix} = \begin{bmatrix} 0 & 0 & 0 & e_{15}(z) & 0 \\ 0 & 0 & e_{24}(z) & 0 & 0 \\ e_{31}(z) & e_{32}(z) & 0 & 0 & 0 \end{bmatrix} \begin{Bmatrix} u_{0,x} - z\, w_{,xx} + f(z)\theta_{x,x} \\ v_{0,y} - z\, w_{,yy} + f(z)\theta_{y,y} \\ f(z)_{,z}\theta_y \\ f(z)_{,z}\theta_x \\ u_{0,y} + v_{0,x} - 2z\, w_{,xy} + f(z)(\theta_{x,y} + \theta_{y,x}) \end{Bmatrix}
$$

$$
+ \begin{bmatrix} \eta_{11}(z) & 0 & 0 \\ 0 & \eta_{22}(z) & 0 \\ 0 & 0 & \eta_{33}(z) \end{bmatrix} \begin{Bmatrix} E_x \\ E_y \\ E_z \end{Bmatrix} + \begin{bmatrix} d_{11}(z) & 0 & 0 \\ 0 & d_{22}(z) & 0 \\ 0 & 0 & d_{33}(z) \end{bmatrix} \begin{Bmatrix} H_x \\ H_y \\ H_z \end{Bmatrix}
$$

$$
\begin{Bmatrix} B_x \\ B_y \\ B_z \end{Bmatrix} = \begin{bmatrix} 0 & 0 & 0 & q_{15}(z) & 0 \\ 0 & 0 & q_{24}(z) & 0 & 0 \\ q_{31}(z) & q_{32}(z) & 0 & 0 & 0 \end{bmatrix} \begin{Bmatrix} u_{0,x} - z\, w_{,xx} + f(z)\theta_{x,x} \\ v_{0,y} - z\, w_{,yy} + f(z)\theta_{y,y} \\ f(z)_{,z}\theta_y \\ f(z)_{,z}\theta_x \\ u_{0,y} + v_{0,x} - 2z\, w_{,xy} + f(z)(\theta_{x,y} + \theta_{y,x}) \end{Bmatrix}
$$

$$
+ \begin{bmatrix} d_{11}(z) & 0 & 0 \\ 0 & d_{22}(z) & 0 \\ 0 & 0 & d_{33}(z) \end{bmatrix} \begin{Bmatrix} E_x \\ E_y \\ E_z \end{Bmatrix} + \begin{bmatrix} \mu_{11}(z) & 0 & 0 \\ 0 & \mu_{22}(z) & 0 \\ 0 & 0 & \mu_{33}(z) \end{bmatrix} \begin{Bmatrix} H_x \\ H_y \\ H_z \end{Bmatrix}
$$

By substitution of Eq. (16) into the equations of motion in Eq. (15), the governing equations can be obtained:

$$\begin{aligned}&A_{11}u_{0,xx} - B_{11}w_{,xxx} + S_{11}\theta_{x,xx} + A_{12}v_{0,yx} - B_{12}w_{,yyx} + S_{12}\theta_{y,yx} + E_{11}\phi_{,x} + F_{11}\psi_{,x}\\&+A_{66}(u_{0,yy} + v_{0,xy}) - 2B_{66}w_{,xyy} + S_{66}(\theta_{x,yy} + \theta_{y,xy}) = I_0\ddot{u} - I_1\ddot{w}_{,x} + I_3\ddot{\theta}_x\end{aligned} \tag{17-1}$$

$$\begin{aligned}&A_{12}u_{0,xy} - B_{12}w_{,xxy} + S_{12}\theta_{x,xy} + A_{22}v_{0,yy} - B_{22}w_{,yyy} + S_{22}\theta_{y,yy} + E_{11}\phi_{,y} + F_{11}\psi_{,y}\\&+A_{66}(u_{0,yx} + v_{0,xx}) - 2B_{66}w_{,xxy} + S_{66}(\theta_{x,yx} + \theta_{y,xx}) = I_0\ddot{v} - I_1\ddot{w}_{,y} + I_3\ddot{\theta}_y\end{aligned} \tag{17-2}$$

$$\begin{aligned}&S_{11}u_{0,xx} - Y_{11}w_{,xxx} + G_{11}\theta_{x,xx} + S_{12}v_{0,yx} - Y_{12}w_{,yyx} + G_{12}\theta_{y,yx} + E_{12}\phi_{,x} + F_{12}\psi_{,x}\\&+S_{66}(u_{0,yy} + v_{0,xy}) - 2Y_{66}w_{,xyy} + G_{66}(\theta_{x,yy} + \theta_{y,xy})\\&-H_{55}\theta_x + J_2\phi_{,x} + J_3\psi_{,x} = I_3\ddot{u} - I_4\ddot{w}_{,x} + I_5\ddot{\theta}_x\end{aligned} \tag{17-3}$$

$$\begin{aligned}&S_{12}u_{0,xy} - Y_{12}w_{,xxy} + G_{12}\theta_{x,xy} + S_{22}v_{0,yy} - Y_{22}w_{,yyy} + G_{22}\theta_{y,yy} + E_{12}\phi_{,y} + F_{12}\psi_{,y}\\&+S_{66}(u_{0,yx} + v_{0,xx}) - 2Y_{66}w_{,xxy} + G_{66}(\theta_{x,yx} + \theta_{y,xx})\\&-H_{44}\theta_y + L_2\phi_{,y} + L_3\psi_{,y} = I_3\ddot{v} - I_4\ddot{w}_{,y} + I_5\ddot{\theta}_y\end{aligned} \tag{17-4}$$

$$\begin{aligned}&B_{11}u_{0,xxx} - D_{11}w_{,xxxx} + Y_{11}\theta_{x,xxx} + B_{12}v_{0,yxx} - D_{12}w_{,yyxx} + Y_{12}\theta_{y,yxx} + E_{22}\phi_{,xx}\\&+F_{22}\psi_{,xx} + B_{12}u_{0,xyy} - D_{12}w_{,xxyy} + Y_{12}\theta_{x,xyy} + B_{22}v_{0,yyy} - D_{22}w_{,yyyy} + Y_{22}\theta_{y,yyy}\\&-4D_{66}w_{,xxyy} + 2\,Y_{66}\left(\theta_{x,yyx} + \theta_{y,xxy}\right) + E_{22}\phi_{,yy} + F_{22}\psi_{,yy} + 2B_{66}\left(u_{0,yyx} + v_{0,xxy}\right)\\&+(N_{Ex} + N_{Mx})\,w_{0,xx} + \left(N_{Ey} + N_{My}\right)w_{0,yy}x - k_w w_0 + k_S\left(w_{0,xx} + w_{0,yy}\right)\\&= I_0\ddot{w} + I_1\left(\ddot{u}_{,x} + \ddot{v}_{,y}\right) - I_2\left(\ddot{w}_{,xx} + \ddot{w}_{,yy}\right) + I_4\left(\ddot{\theta}_{x,x} + \ddot{\theta}_{y,y}\right)\end{aligned} \tag{17-5}$$

$$\begin{aligned}&J_2\theta_{x,x} + Q_1\phi_{,xx} + Q_2\psi_{,xx} + L_2\theta_{y,y} + X_1\phi_{,yy} + X_2\psi_{,yy}\\&E_{11}(u_{0,x} + v_{0,y}) - E_{22}(w_{,xx} + w_{,yy}) + E_{12}(\theta_{x,x} + \theta_{y,y}) - P_1\phi - P_2\psi = 0\end{aligned} \tag{17-6}$$

$$\begin{aligned}&J_3\theta_{x,x} + Q_2\phi_{,xx} + Q_3\psi_{,xx} + L_3\theta_{y,y} + X_2\phi_{,yy} + X_3\psi_{,yy}\\&F_{11}(u_{0,x} + v_{0,y}) - F_{22}(w_{,xx} + w_{,yy}) + F_{12}(\theta_{x,x} + \theta_{y,y}) - P_2\phi - P_3\psi = 0\end{aligned} \tag{17-7}$$

Where

$$A_{11}, B_{11}, D_{11}, S_{11}, Y_{11}, G_{11} = \int_{-h/2}^{h/2} C_{11}(z)(1, z, z^2, f(z), zf(z), f^2(z))dz \qquad H_{44} = \int_{-h/2}^{h/2} C_{44}(z)\, f^2(z)_{,z}\, dz$$

$$A_{12}, B_{12}, D_{12}, S_{12}, Y_{12}, G_{12} = \int_{-h/2}^{h/2} C_{12}(z)(1, z, z^2, f(z), zf(z), f^2(z))dz \qquad H_{55} = \int_{-h/2}^{h/2} C_{55}(z)\, f^2(z)_{,z}\, dz$$

$$A_{22}, B_{22}, D_{22}, S_{22}, Y_{22}, G_{22} = \int_{-h/2}^{h/2} C_{22}(z)(1, z, z^2, f(z), zf(z), f^2(z))dz \qquad J_2 = \int_{-h/2}^{h/2} e_{15}(z)\mathrm{Cos}\left(\frac{\pi}{h}z\right) f(z)_{,z}\, dz$$

$$A_{66}, B_{66}, D_{66}, S_{66}, Y_{66}, G_{66} = \int_{-h/2}^{h/2} C_{66}(z)(1, z, z^2, f(z), zf(z), f^2(z))dz \qquad J_3 = \int_{-h/2}^{h/2} q_{15}(z)\mathrm{Cos}\left(\frac{\pi}{h}z\right) f(z)_{,z}dz$$

$$E_{11}, E_{12}, E_{22} = \int_{-h/2}^{h/2} e_{31}(z)\left(\frac{\pi}{h}\right)\mathrm{Sin}\left(\frac{\pi}{h}z\right)(1, f(z), z)dz \qquad L_2 = \int_{-h/2}^{h/2} e_{24}(z)\mathrm{Cos}\left(\frac{\pi}{h}z\right) f(z)_{,z}dz$$

$$F_{11}, F_{12}, F_{22} = \int_{-h/2}^{h/2} q_{31}(z)\left(\frac{\pi}{h}\right)\mathrm{Sin}\left(\frac{\pi}{h}z\right)(1, f(z), z)dz \qquad L_3 = \int_{-h/2}^{h/2} q_{24}(z)\mathrm{Cos}\left(\frac{\pi}{h}z\right) f(z)_{,z}dz$$

$$Q_1 = \int_{-h/2}^{h/2} \eta_{11}(z)\left[\mathrm{Cos}\left(\frac{\pi}{h}z\right)\right]^2 dz \qquad Q_2 = \int_{-h/2}^{h/2} d_{11}(z)\left[\mathrm{Cos}\left(\frac{\pi}{h}z\right)\right]^2 dz$$

$$X_1 = \int_{-h/2}^{h/2} \eta_{22}(z)\left[\mathrm{Cos}\left(\frac{\pi}{h}z\right)\right]^2 dz \qquad X_2 = \int_{-h/2}^{h/2} d_{22}(z)\left[\mathrm{Cos}\left(\frac{\pi}{h}z\right)\right]^2 dz$$

$$P_1 = \int_{-h/2}^{h/2} \eta_{33}(z)\left[\left(\frac{\pi}{h}\right)\mathrm{Sin}\left(\frac{\pi}{h}z\right)\right]^2 dz \qquad P_2 = \int_{-h/2}^{h/2} d_{33}(z)\left[\left(\frac{\pi}{h}\right)\mathrm{Sin}\left(\frac{\pi}{h}z\right)\right]^2 dz$$

$$Q_3 = \int_{-h/2}^{h/2} \mu_{11}(z)\left[\mathrm{Cos}\left(\frac{\pi}{h}z\right)\right]^2 dz \qquad X_3 = \int_{-h/2}^{h/2} \mu_{22}(z)\left[\mathrm{Cos}\left(\frac{\pi}{h}z\right)\right]^2 dz$$

$$P_3 = \int_{-h/2}^{h/2} \mu_{33}(z) \left[\left(\frac{\pi}{h}\right) \mathrm{Sin}\left(\frac{\pi}{h} z\right)\right]^2 dz$$

FSDT

According to Eq. (13), forces and momentums are defined as follows:

$$\begin{Bmatrix} N_x \\ N_y \\ N_{xy} \end{Bmatrix} = \int_{h/2}^{-h/2} \begin{Bmatrix} \sigma_x \\ \sigma_y \\ \tau_{xy} \end{Bmatrix} dz \quad \begin{Bmatrix} M_x \\ M_y \\ M_{xy} \end{Bmatrix} = \int_{h/2}^{-h/2} \begin{Bmatrix} \sigma_x \\ \sigma_y \\ \tau_{xy} \end{Bmatrix} z dz$$
$$\begin{Bmatrix} Q_x \\ Q_y \end{Bmatrix} = k \int_{h/2}^{-h/2} \begin{Bmatrix} \tau_{xz} \\ \tau_{yz} \end{Bmatrix} dz \quad \begin{Bmatrix} I_0 \\ I_1 \\ I_2 \end{Bmatrix} = \int_{h/2}^{-h/2} \begin{Bmatrix} 1 \\ z \\ z^2 \end{Bmatrix} \rho(z)\, dz \tag{18}$$

The governing equations of motion for the rectangular plate are expressed as follows:

$$\begin{aligned}
&N_{x,x} + N_{xy,y} = I_0 \ddot{u} + I_1 \ddot{\theta}_x \\
&N_{y,y} + N_{xy,x} = I_0 \ddot{v} + I_1 \ddot{\theta}_y \\
&M_{x,x} + M_{xy,y} - Q_x = I_1 \ddot{u} + I_2 \ddot{\theta}_x \\
&M_{y,y} + M_{xy,x} - Q_y = I_1 \ddot{v} + I_2 \ddot{\theta}_y \\
&Q_{x,x} + Q_{y,y} + q = I_0 \ddot{w} \\
&\int_{z_k}^{z_{k+1}} \left(\frac{\partial D_x}{\partial x} \mathrm{Cos}(\frac{\pi z}{h}) + \frac{\partial D_y}{\partial y} \mathrm{Cos}(\frac{\pi z}{h}) + \frac{\pi}{h} D_z \mathrm{Sin}(\frac{\pi z}{h})\right) dz = 0 \\
&\int_{z_k}^{z_{k+1}} \left(\frac{\partial B_x}{\partial x} \mathrm{Cos}(\frac{\pi z}{h}) + \frac{\partial B_y}{\partial y} \mathrm{Cos}(\frac{\pi z}{h}) + \frac{\pi}{h} B_z \mathrm{Sin}(\frac{\pi z}{h})\right) dz = 0
\end{aligned} \tag{19}$$

By substituting the displacement from Eq. (4) into the strain of Eq. (5) and rewriting Eq. (19), we have:

$$\begin{Bmatrix} N_x \\ N_y \\ N_{xy} \end{Bmatrix} = \int_{z_k}^{z_{k+1}} \begin{bmatrix} c_{11}(z) & c_{12}(z) & 0 \\ c_{12}(z) & c_{22}(z) & 0 \\ 0 & 0 & c_{66}(z) \end{bmatrix} \begin{Bmatrix} u_{0,x} + z\theta_{x,x} \\ v_{0,y} + z\theta_{y,y} \\ u_{0,y} + v_{0,x} + z(\theta_{x,y} + \theta_{y,x}) \end{Bmatrix} dz$$
$$- \int_{z_k}^{z_{k+1}} \begin{bmatrix} 0 & 0 & e_{31}(z) \\ 0 & 0 & e_{32}(z) \\ 0 & 0 & 0 \end{bmatrix} \begin{Bmatrix} 0 \\ 0 \\ -\phi_{,z} \end{Bmatrix} dz - \int_{z_k}^{z_{k+1}} \begin{bmatrix} 0 & 0 & q_{31}(z) \\ 0 & 0 & q_{32}(z) \\ 0 & 0 & 0 \end{bmatrix} \begin{Bmatrix} 0 \\ 0 \\ -\psi_{,z} \end{Bmatrix} dz$$

$$\begin{Bmatrix} Q_y \\ Q_x \end{Bmatrix} = k \int_{z_k}^{z_{k+1}} \begin{bmatrix} c_{44}(z) & 0 \\ 0 & c_{55}(z) \end{bmatrix} \begin{Bmatrix} w_{0,y} + \theta_y \\ w_{0,x} + \theta_x \end{Bmatrix} dz$$
$$- \int_{z_k}^{z_{k+1}} \begin{bmatrix} e_{24}(z) & 0 \\ 0 & e_{15}(z) \end{bmatrix} \begin{Bmatrix} E_y \\ E_x \end{Bmatrix} dz - \int_{z_k}^{z_{k+1}} \begin{bmatrix} q_{24}(z) & 0 \\ 0 & q_{15}(z) \end{bmatrix} \begin{Bmatrix} H_y \\ H_x \end{Bmatrix} dz$$

$$\begin{Bmatrix} M_x \\ M_y \\ M_{xy} \end{Bmatrix} = \int_{z_k}^{z_{k+1}} \begin{bmatrix} c_{11}(z) & c_{12}(z) & 0 \\ c_{12}(z) & c_{22}(z) & 0 \\ 0 & 0 & c_{66}(z) \end{bmatrix} \begin{Bmatrix} u_{0,x} + z\theta_{x,x} \\ v_{0,y} + z\theta_{y,y} \\ u_{0,y} + v_{0,x} + z(\theta_{x,y} + \theta_{y,x}) \end{Bmatrix} z dz$$
$$- \int_{z_k}^{z_{k+1}} \begin{bmatrix} 0 & 0 & e_{31}(z) \\ 0 & 0 & e_{32}(z) \\ 0 & 0 & 0 \end{bmatrix} \begin{Bmatrix} 0 \\ 0 \\ -\phi_{,z} \end{Bmatrix} z dz - \int_{z_k}^{z_{k+1}} \begin{bmatrix} 0 & 0 & q_{31}(z) \\ 0 & 0 & q_{32}(z) \\ 0 & 0 & 0 \end{bmatrix} \begin{Bmatrix} 0 \\ 0 \\ -\psi_{,z} \end{Bmatrix} z dz \tag{20}$$

$$\begin{Bmatrix} D_x \\ D_y \\ D_z \end{Bmatrix} = \begin{bmatrix} 0 & 0 & 0 & e_{15}(z) & 0 \\ 0 & 0 & e_{24}(z) & 0 & 0 \\ e_{31}(z) & e_{32}(z) & 0 & 0 & 0 \end{bmatrix} \begin{Bmatrix} u_{0,x} + z\theta_{x,x} \\ v_{0,y} + z\theta_{y,y} \\ w_{0,y} + \theta_y \\ w_{0,x} + \theta_x \\ u_{0,y} + v_{0,x} + z(\theta_{x,y} + \theta_{y,x}) \end{Bmatrix}$$
$$+ \begin{bmatrix} \eta_{11}(z) & 0 & 0 \\ 0 & \eta_{22}(z) & 0 \\ 0 & 0 & \eta_{33}(z) \end{bmatrix} \begin{Bmatrix} E_x \\ E_y \\ E_z \end{Bmatrix} + \begin{bmatrix} d_{11}(z) & 0 & 0 \\ 0 & d_{22}(z) & 0 \\ 0 & 0 & d_{33}(z) \end{bmatrix} \begin{Bmatrix} H_x \\ H_y \\ H_z \end{Bmatrix}$$

$$\begin{Bmatrix} B_x \\ B_y \\ B_z \end{Bmatrix} = \begin{bmatrix} 0 & 0 & 0 & q_{15}(z) & 0 \\ 0 & 0 & q_{24}(z) & 0 & 0 \\ q_{31}(z) & q_{32}(z) & 0 & 0 & 0 \end{bmatrix} \begin{Bmatrix} u_{0,x} + z\theta_{x,x} \\ v_{0,y} + z\theta_{y,y} \\ w_{0,y} + \theta_y \\ w_{0,x} + \theta_x \\ u_{0,y} + v_{0,x} + z(\theta_{x,y} + \theta_{y,x}) \end{Bmatrix}$$
$$+ \begin{bmatrix} d_{11}(z) & 0 & 0 \\ 0 & d_{22}(z) & 0 \\ 0 & 0 & d_{33}(z) \end{bmatrix} \begin{Bmatrix} E_x \\ E_y \\ E_z \end{Bmatrix} + \begin{bmatrix} \mu_{11}(z) & 0 & 0 \\ 0 & \mu_{22}(z) & 0 \\ 0 & 0 & \mu_{33}(z) \end{bmatrix} \begin{Bmatrix} H_x \\ H_y \\ H_z \end{Bmatrix}$$

By substitution of Eq. (20) into the equations of motion in Eq. (19), the governing equations will be obtained as follows:

$$A_{11}u_{0,xx} + B_{11}\theta_{x,xx} + A_{12}v_{0,yx} + B_{12}\theta_{y,yx} + E_{11}\phi_{,x} + F_{11}\psi_{,x} + A_{66}(u_{0,yy} + v_{0,xy}) + B_{66}(\theta_{x,yy} + \theta_{y,xy}) = I_0u_{0,tt} + I_1\theta_{x,tt} \tag{21-1}$$

$$A_{12}u_{0,xy} + B_{12}\theta_{x,xy} + A_{22}v_{0,yy} + B_{22}\theta_{y,yy} + A_{66}(u_{0,yx} + v_{0,xx}) + B_{66}(\theta_{x,yx} + \theta_{y,xx}) + G_{11}\phi_{,y} + H_{11}\psi_{,y} = I_0v_{0,tt} + I_1\theta_{y,tt} \tag{21-2}$$

$$B_{11}u_{0,xx} + D_{11}\theta_{x,xx} + B_{12}v_{0,yx} + D_{12}\theta_{y,yx} + B_{66}(u_{0,yy} + v_{0,xy}) + D_{66}(\theta_{x,yy} + \theta_{y,xy}) - KA_{55}(w_{0,x} + \theta_x) + (E_{22} + KJ_2)\phi_{,x} + (F_{22}KJ_3)\psi_{,x} = I_1u_{0,tt} + I_2\theta_{x,tt} \tag{21-3}$$

$$B_{12}u_{0,xy} + D_{12}\theta_{x,xy} + B_{22}v_{0,yy} + D_{22}\theta_{y,yy} + B_{66}(u_{0,yx} + v_{0,xx}) + D_{66}(\theta_{x,yx} + \theta_{y,xx}) - KA_{44}(w_{0,y} + \theta_y) + (G_{22} + KL_2)\phi_{,y} + (H_{22}KL_3)\psi_{,y} = I_1v_{0,tt} + I_2\theta_{y,tt} \tag{21-4}$$

$$KA_{44}(w_{0,yy} + \theta_{y,y}) + KA_{55}(w_{0,xx} + \theta_{x,x}) - KL_2\phi_{,yy} - KL_3\psi_{,yy} - KJ_2\phi_{,xx} - KJ_3\psi_{,xx} - k_ww_0 + k_S(w_{0,xx} + w_{0,yy}) + (N_{Ex} + N_{Mx})w_{0,xx} + (N_{Ey} + N_{My})w_{0,yy} = I_0W_{0,tt} \tag{21-5}$$

$$J_2(w_{0,xx} + \theta_{x,x}) + Q_1\phi_{,xx} + Q_2\psi_{,xx} + L_2(w_{0,yy} + \theta_{y,y}) + X_1\phi_{,yy} + X_2\psi_{,yy} \quad E_{11}u_{0,x} + G_{11}v_{0,y} + E_{22}\theta_{x,x} + G_{22}\theta_{y,y} - P_1\phi - P_2\psi = 0 \tag{21-6}$$

$$J_3(w_{0,xx} + \theta_{x,x}) + Q_2\phi_{,xx} + Q_3\psi_{,xx} + L_3(w_{0,yy} + \theta_{y,y}) + X_2\phi_{,yy} + X_3\psi_{,yy} \quad F_{11}u_{0,x} + H_{11}v_{0,y} + F_{22}\theta_{x,x} + H_{22}\theta_{y,y} - P_2\phi - P_3\psi = 0 \tag{21-7}$$

Where

$$A_{44} = \int_{-h/2}^{h/2} C_{44}(z)dz \qquad A_{55} = \int_{-h/2}^{h/2} C_{55}(z)dz$$

$$G_{11}, G_{22} = \int_{-h/2}^{h/2} e_{32}(z)\left(\frac{\pi}{h}\right)\mathrm{Sin}\left(\frac{\pi}{h}z\right)(1, z)dz \qquad H_{11}, H_{22} = \int_{-h/2}^{h/2} q_{32}(z)\left(\frac{\pi}{h}\right)\mathrm{Sin}\left(\frac{\pi}{h}z\right)(1, z)dz$$

$$N_x^E = \int_{-h/2}^{h/2} 2e_{31}(z)\frac{\phi_0}{h}dz \qquad N_x^M = \int_{-h/2}^{h/2} 2q_{31}(z)\frac{\psi_0}{h}dz$$

$$N_y^E = \int_{-h/2}^{h/2} 2e_{32}(z)\frac{\phi_0}{h}dz \qquad N_y^M = \int_{-h/2}^{h/2} 2q_{32}(z)\frac{\psi_0}{h}dz$$

$$J_2 = \int_{-h/2}^{h/2} e_{15}(z)\mathrm{Cos}\left(\frac{\pi}{h}z\right)dz \qquad J_3 = \int_{-h/2}^{h/2} q_{15}(z)\mathrm{Cos}\left(\frac{\pi}{h}z\right)dz$$

$$L_2 = \int_{-h/2}^{h/2} e_{24}(z)\mathrm{Cos}\left(\frac{\pi}{h}z\right)dz \qquad L_3 = \int_{-h/2}^{h/2} q_{24}(z)\mathrm{Cos}\left(\frac{\pi}{h}z\right)dz$$

SOLUTION METHOD

In this section, Navier's method is utilized to solve the linear and coupled governing equations for FGMEE, which were obtained in Eqs. (17 and 21). The simply-supported boundary conditions for in-plane vibrations of the rectangular plate are as follows [40]:

$$\begin{aligned} u_0 = N_y = 0 \qquad & at \quad (y = 0, b) \\ v_0 = N_x = 0 \qquad & at \quad (x = 0, a) \end{aligned} \tag{22-1}$$

Besides, simply-supported boundary conditions for out-of-plane vibrations of a rectangular plate are expressed as follows [41]:

$$\begin{aligned} w_0 = \theta_x = M_y = 0 \qquad & at \quad (y = 0, b) \\ w_0 = \theta_y = M_x = 0 \qquad & at \quad (x = 0, a) \end{aligned} \tag{22-2}$$

To solve the obtained governing differential equations, the responses satisfying the aforementioned boundary conditions are considered [32]:

$$\begin{aligned} u_0(x,y,t) &= \sum_{n=1}^{\infty}\sum_{m=1}^{\infty} U_{nm}\,\mathrm{Cos}(\alpha x)\mathrm{Sin}(\beta y)e^{i\omega t} \\ v_0(x,y,t) &= \sum_{n=1}^{\infty}\sum_{m=1}^{\infty} V_{nm}\,\mathrm{Sin}(\alpha x)\mathrm{Cos}(\beta y)e^{i\omega t} \\ w_0(x,y,t) &= \sum_{n=1}^{\infty}\sum_{m=1}^{\infty} W_{nm}\,\mathrm{Sin}(\alpha x)\mathrm{Sin}(\beta y)e^{i\omega t} \\ \theta_x(x,y,t) &= \sum_{n=1}^{\infty}\sum_{m=1}^{\infty} X_{nm}\,\mathrm{Cos}(\alpha x)\mathrm{Sin}(\beta y)e^{i\omega t} \\ \theta_y(x,y,t) &= \sum_{n=1}^{\infty}\sum_{m=1}^{\infty} Y_{nm}\,\mathrm{Sin}(\alpha x)\mathrm{Cos}(\beta y)e^{i\omega t} \\ \phi(x,y,t) &= \sum_{n=1}^{\infty}\sum_{m=1}^{\infty} \phi_{nm}\,\mathrm{Sin}(\alpha x)\mathrm{Sin}(\beta y)e^{i\omega t} \\ \psi(x,y,t) &= \sum_{n=1}^{\infty}\sum_{m=1}^{\infty} \psi_{nm}\,\mathrm{Sin}(\alpha x)\mathrm{Sin}(\beta y)e^{i\omega t} \\ \alpha = \frac{m\pi}{a} \qquad & \beta = \frac{n\pi}{b} \end{aligned} \tag{23}$$

The natural frequencies of the system can be obtained in an Eigen-value form by substitution of Eqs. (23) into Eqs. (17 and 21):

$$\{[K] - [M]\omega^2\}[q] = 0 \tag{24}$$

where M and K are mass and stiffness matrices, respectively, and q denotes the displacement vector defined as follows:

$$q = [U \quad V \quad X \quad Y \quad W \quad \varphi \quad \psi]^T \tag{25}$$

RESULTS AND DISCUSSION

In this section, the numerical results are calculated for the in-plane and out-of-plane vibrations of the plate.

In-plane Vibrations

To validate the obtained results for in-plane vibrations, the natural frequencies attained for in-plane vibrations of the isotropic plate were compared with the results of reference [5] and [15], based on the third-order shear deformation theory and 3-D elastic theory, respectively. As it is evident, good consistency was achieved confirming the validity of the obtained results.

Table 1. Comparison of non-dimensional in-plane natural frequencies $\chi = \frac{\omega a}{\pi}\sqrt{\frac{\rho}{G}}$ for isotropic rectangular plates

Theory	Mode sequences					
	(0,1)	(1,0)	(1, 1)	(0,2)	(1,2)	(2,0)
Elasticity [15]	0.833	1.0000	1.301	1.6667	1.9437	2.0000
TSDT [5]	0.833	1.0000	1.301	1.6667	1.9437	2.0000
Present study	0.833	1.0000	1.301	1.6666	1.9436	2.0000

Out-of-plane Vibrations

Table 2 compares our results for the out-of-plane natural frequencies of an isotropic plate with simply-supported boundary conditions with the results of reference [1] and references [2, 3, 4], based on the 3-D elastic theory and third-order shear deformation theory, respectively.

Table 2. Comparison of non-dimensional out-of-plane natural frequencies $\chi = \omega h\sqrt{\frac{\rho}{G}}$ for SSSS isotropic rectangular plates

Theory	Mode sequences					
	(1,1)	(1,2)	(1,3)	(2,2)	(2,3)	(3,3)
3-D [1]	0.0932	0.226	0.4171	0.3421	0.5239	0.6889
TSDT [3]	0.0931	0.2222	0.4158	0.3411	0.5221	0.6862
TSDT [4]	0.0930	0.2220	0.4151	0.3406	0.5208	0.6840
TSDT [2]	0.0930	0.2220	0.4151	0.3406	0.5208	0.6840
Present study	0.0894	0.2139	0.4013	0.3290	0.5043	0.6636

Table 3 also presents a comparison of the out-of-plane natural frequencies of a plate with simply-supported boundary conditions with a transversely isotropic plate based on shear deformation theory [5].

Table 3. Non-dimensional out-of-plane natural frequencies $\chi = \frac{\omega a^2}{h}\sqrt{\frac{\rho}{G}}$ of transversely isotropic plates (SSSS)

Theory	Mode sequences				
	(1,1)	(1,2)	(2,1)	(2,2)	(1,3)
FSDT [5]	9.6016	23.8923	23.8923	38.0519	47.4202
Present study	9.2311	23.0308	23.0308	36.7747	45.9065

Moreover, to validate the vibration of MEE plates based on FSDT, the out-of-plane non-dimensional natural frequencies, $\chi = \frac{\omega a^2}{h}\sqrt{\frac{\rho}{c_{11}}}$, obtained in this study were compared with results published by Li and Zhang [41] in Figure 3 of their paper. As it is clear, there is a proper agreement between these studies.

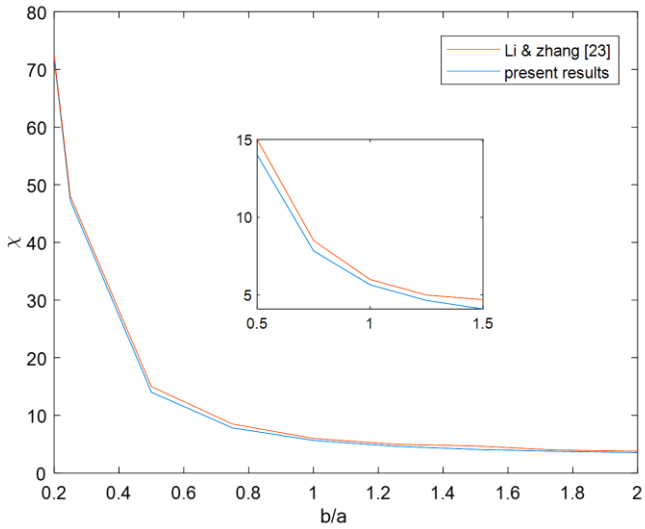

Figure 3. Comparison of normalized frequency $\boldsymbol{h = 0.01\ \varphi = 0\ n = m = 1}$

In-plane and out-of-plane Vibrations

To validate the results of the present work for the MEE plate based on ESDT and FSDT, a comparison was made with the results reported by Ke et al. [24] for the classical theory of MEE nanoplate. Table 4 provides the result of this comparison for non-dimensional natural frequencies which suggests a good coincidence.

Table 4. Comparison of non-dimensional nature frequency $\boldsymbol{\chi = \omega\, a\sqrt{\frac{I_0}{A_{11}}}}$ MEE plate $\boldsymbol{\psi_0 = \varphi_0 = 0}$

	Work	ω_{11}	ω_{12}	ω_{22}
$\boldsymbol{a = b = 60nm}$ $\boldsymbol{h = 4nm}$	Present study (ESDT)	0.3698	0.89	1.40
	Present study (FSDT)	0.3698	0.8861	1.384
	Ke et al [24]	0.3698	0.9247	1.48

This section is dedicated to the numerical examples of out-of-plane vibrations of the FG-MEE rectangular plate. The bottom and top of the plate were considered to be made of $CoFe_2O_4$ and $BaTiO_3$, respectively. Properties of FG-MEE material are listed in Table 5.

Table 5. Properties of Materials [30]

Properties	BaTiO3	CoFe2O4	Properties	BaTiO3	CoFe2O4
$\boldsymbol{C_{11} = C_{22}}$ $\boldsymbol{(Gpa)}$	166	286	$q_{31} = q_{32}$ (N/MA)	0	580.3
$\boldsymbol{C_{12}}$	77	173	$q_{24} = q_{15}$	0	550
$\boldsymbol{C_{13} = C_{23}}$	78	170.5	q_{33}	0	699.7
$\boldsymbol{C_{33}}$	162	269.5	$\eta_{11} = \eta_{22}$ $(10^{-9}\ C^2/Nm^2)$	11.2	0.08
$\boldsymbol{C_{44} = C_{55}}$	43	45.3	η_{33}	12.6	0.093
$\boldsymbol{C_{66}}$	44.5	56.5	$d_{11} = d_{22} = d_{33}$	0	0
$\boldsymbol{e_{31} = e_{32}}$ $\boldsymbol{(C/m^2)}$	-4.4	0	$\mu_{11} = \mu_{22}$ $(10^{-6}\ NS^2/C^2)$	5	-590
$\boldsymbol{e_{24} = e_{15}}$	11.6	0	μ_{33}	10	157
$\boldsymbol{e_{33}}$	18.6	0	$\rho\ (kg/m^3)$	5800	5300

First, the effects of different parameters, including electrical and magnetic potentials, as well as the plate length, on the natural frequencies were investigated. Thickness was considered as a function of length, while the thickness-to-length

ratio was assumed to be 0.1. Table 6 shows the effect of length variations with positive, zero, and negative electrical potentials on the natural frequencies in two modes of out-of-plane vibrations and coupled in-plane and out-of-plane vibrations. As can be seen, the natural frequency decreases by increasing the electrical potential. Also, the effect of plate length was investigated on the natural frequencies in two modes of out-of-plane vibration and coupled in-plane and out-of-plane vibrations, based on FSDT theory as plotted in Figure 4. The natural frequencies decrease by the increment of the rectangular plate length. The maximum effect of electrical potential on natural frequency was observed by 2.5-time enhancing the length of the initial length.

Table 6. Effect of electrical potential on the natural frequency $\frac{h}{a} = 0.1 \quad p = n = m = 1$

a	Theory	In-plane and Out-of-plane			Out-of-plane		
		$\varphi = -10^7(V)$	$\varphi = 0$	$\varphi = 10^7(V)$	$\varphi = -10^7(V)$	$\varphi = 0$	$\varphi = 10^7(V)$
1	FSDT	3637.12	3418.41	3184.71	3672.64	3456.06	3224.97
	ESDT	3638.38	3419.76	3186.16	3673.91	3457.41	3226.43
2	FSDT	1764.73	1709.21	1651.81	1782.34	1728.02	1671.21
	ESDT	1765.38	1709.88	1652.51	1783.65	1728.71	1671.96
3	FSDT	1164.28	1139.47	1114.11	1176.67	1151.98	1126.94
	ESDT	1164.72	1139.92	1114.57	1177.02	1152.47	1127.39

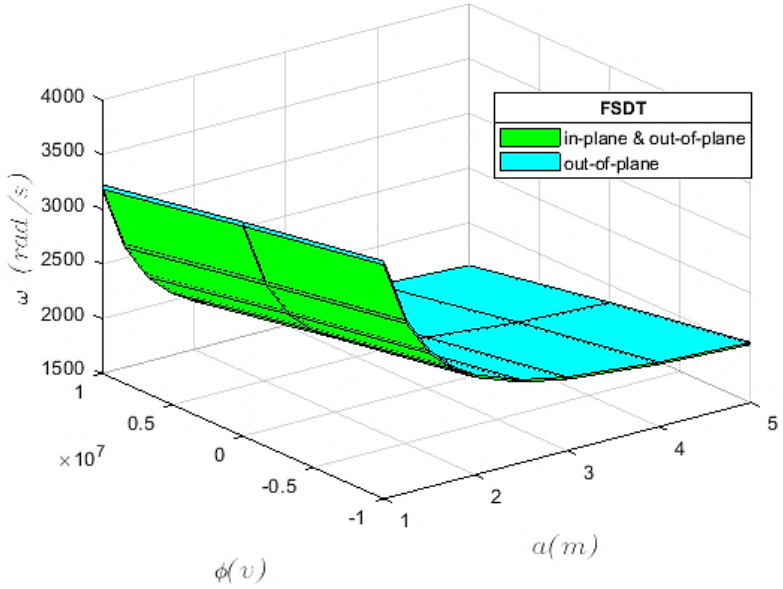

Figure 4. Effect of electrical potential and length on the natural frequency $\frac{h}{a} = 0.1 \quad p = n = m = 1$

Due to the inherent negative piezoelectric coefficient of MEE materials, application of the negative electrical potential to the plate can lead to an increase in the natural frequency; whilst, a decrease in the natural frequency is probable upon applying a positive electrical potential. In other words, by imposing a positive/negative external electric potential on the FG-MEE plate, compressive/tensile in-plane loads will be generated resulting in a subsequent reduction/enhancement of the natural frequency.

The effect of length variations with positive, zero, and negative magnetic potentials on the natural frequency is listed in Table 7 for two modes of out-of-plane vibration and coupled in-plane and out-of-plane vibrations. This table suggests n increasing trend of frequency by elevating the magnetic potential.

Table 7. Effect of magnetic potentials on the natural frequency $\frac{h}{a} = 0.1 \quad p = n = m = 1$

a	Theory	In-plane and Out-of-plane			Out-of-plane		
		$\psi = -10^5(A)$	$\psi = 0$	$\psi = 10^5(A)$	$\psi = -10^5(A)$	$\psi = 0$	$\psi = 10^5(A)$
1	FSDT	3106.5	3418.41	3704.15	3147.72	3456.06	3738.87
	ESDT	3107.98	3419.76	3705.38	3149.21	3457.41	3740.3
2	FSDT	1633.09	1709.21	1782.07	1652.80	1728.02	1800.06
	ESDT	1633.8	1709.88	1782.72	1653.45	1728.71	1800.82
3	FSDT	1105.9	1139.47	1172.08	1118.75	1151.98	1184.17
	ESDT	1106.36	1139.92	1172.51	1119.27	1152.47	1184.74

Furthermore, the effect of plate length on the natural frequencies is depicted in Figure 5 for two modes of out-of-plane vibration and coupled in-plane and out-of-plane vibrations, based on the ESDT theory. The natural frequencies decreased by incrementing the rectangular plate length. The maximum effect of magnetic potential on natural frequency was observed by the 1.5-fold increase of the initial length. By reviewing both graphs, an insignificant difference can be observed between natural frequencies in two modes of coupled in-plane and out-of-plane vibrations and out-of-plane vibrations, so the in-plane vibrations can be ignored in the analysis.

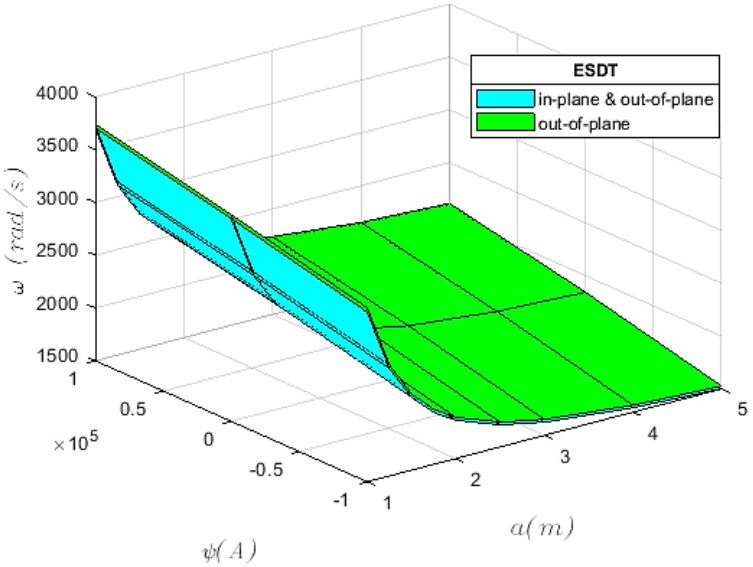

Figure 5. Effect of electrical potential and length on the natural frequency $\frac{h}{a} = 0.1 \quad p = n = m = 1$

Therefore, it can be declared that imposing the negative/ positive applied external magnetic potential will generate tensile/compressive in-plane loads in the FG-MEE plate resulting in the consequent frequency increase/reduction.

Table 8. Effect of electrical potential on the natural frequency

h	Theory	In-plane and Out-of-plane			Out-of-plane		
		$\varphi = -10^7(V)$	$\varphi = 0$	$\varphi = 10^7(V)$	$\varphi = -10^7(V)$	$\varphi = 0$	$\varphi = 10^7(V)$
0.1	FSDT	3637.12	3418.41	3184.71	3672.64	3456.06	3224.97
	ESDT	3638.38	3419.76	3186.16	3673.91	3457.41	3226.43
0.2	FSDT	6075.28	6012.8	5949.66	8929.87	8973.58	9017.07
	ESDT	6087.12	6024.79	5961.80	8754.47	8798.99	8843.29
0.3	FSDT	7769.14	7737	7704.73	9049.55	9078.32	9107.01
	ESDT	7809.93	7778.01	7745.95	8825.37	8854.80	8884.13

In the latter case, the length and width were kept constant while the thickness was increased. Table 8 shows the effect of thickness variation at negative, zero, and positive electrical potential in two modes of out-of-plane, coupled in-plane and out-of-plane vibrations. As can be seen, an increase in the electrical potential declined the natural frequencies; moreover, an increment in the plate thickness enhanced the natural frequencies. Moreover, the effect of thickness variations at positive, zero, and negative magnetic potential is showed in Table 9 on the natural frequency in both modes of out-of-plane and coupled in-plane and out-of-plane vibrations. According to this table, an enhancement of the magnetic potential and plate thickness resulted in an increment of natural frequencies. A comparison between the two theories suggests an increase in the frequency difference by enlarging the thickness.

Table 9. Effect of magnetic potentials on the natural frequency

h	Theory	In-plane and Out-of-plane			Out-of-plane		
		$\psi = -10^5(A)$	$\psi = 0$	$\psi = 10^5(A)$	$\psi = -10^5(A)$	$\psi = 0$	$\psi = 10^5(A)$
0.1	FSDT	3106.5	3418.41	3704.15	3147.72	3456.06	3738.87
	ESDT	3107.98	3419.76	3705.38	3149.21	3457.41	3740.3
0.2	FSDT	5929.38	6012.8	6095.06	9030.89	8973.58	8915.89
	ESDT	5941.58	6024.79	6106.87	8857.37	8798.99	8740.22
0.3	FSDT	7694.41	7737	7779.36	9116.14	9078.32	9040.35
	ESDT	7735.7	7778.01	7820.08	8893.46	8854.80	8815.97

The effect of the power-law index on natural frequencies is illustrated in Figure 6 for zero electrical and magnetic potentials. As can be seen, by increasing the power index, natural frequencies raised. Moreover, a comparison between the two theories shows that although the frequency difference increased with the increment of thickness; this difference declined by the increase of the power index.

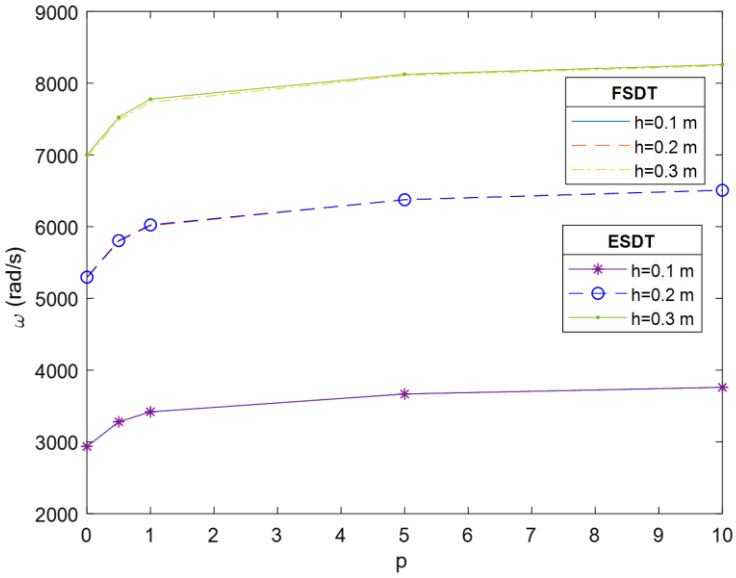

Figure 6. Effect of power index on the natural frequency

In Table 10, the natural frequency of FGMEE plates with different thicknesses is shown for different types of elastic media, for FSDT and ESDT. Here, three types of the elastic foundation were considered: without elastic medium ($k_w = k_S = 0$), Winkler medium ($k_w \neq 0, k_S = 0$), and Pasternak medium ($k_w = k_S \neq 0$). It can be seen that the natural frequency of the Pasternak medium was lower than Winkler as the Pasternak medium considers spring and shear constant as well as a higher structure stiffness. However, an increment of the plate thickness increased the plate stiffness, hence reducing the effect of the Pasternak medium on the natural frequency.

Table 10. The natural frequency of FGMEE plates with different types of elastic media

h	Theory	In-plane and Out-of-plane		
		Without elastic medium	With Winkler medium	With Pasternak medium
0.1	FSDT	3418.41	3416.33	3375.02
	ESDT	3419.76	3417.68	3376.38
0.2	FSDT	6012.8	6012.22	6000.79
	ESDT	6024.79	6024.21	6012.81
0.3	FSDT	7737	7736.7	7730.85
	ESDT	7778.01	7777.71	7771.89

CONCLUSIONS

In this paper, in-plane and out-of-plane free vibrations of the FG-MEE rectangular plate was investigated using FSDT and ESDT. The variations of electric and magnetic potentials along the thickness of the plate were determined according to the Maxwell equation and magnetoelectric boundary conditions. The following conclusions can be made from the obtained numerical results:

1) The natural frequency difference between the coupling mode and out-of-plane vibration mode at a thickness of 0.1m is about 1.1%. With increasing the thickness to 0.2 this value reached 49.2%.
2) The natural frequency difference between the two theories increased with enhancing the plate thickness. This difference with the thickness-to-length ratio of 0.1 is 0.03%. When the aspect ratio was set to 0.2 and 0.3 these differences reached 0.2% and 0.5%, respectively.
3) In the FG-MEE plate, an increase in the power index from zero to 0.5 resulted in the highest frequency enhancement (11.7%). Moreover, with the increasing plate thickness, this value decreased and reached 7.4%.
4) The natural frequency of vibration increased/decreased with positive/negative electrical potential for the FG-MEE plate.
5) Natural frequency decreased/increased with positive/negative magnetic potentials in the FG-MEE rectangular plate.
6) In the FG-MEE plate, the effect of the Pasternak medium on the reduction of the natural frequency declined from 1.3% to 0.08% when the plate thickness was incremented.

REFERENCES

[1] S. Srinivas, C. J. Rao, and A. Rao, "An exact analysis for vibration of simply-supported homogeneous and laminated thick rectangular plates," *Journal of sound and vibration,* vol. 12, no. 2, pp. 187-199, 1970.

[2] J. Reddy and N. Phan, "Stability and vibration of isotropic, orthotropic and laminated plates according to a higher-order shear deformation theory," *Journal of sound and vibration,* vol. 98, no. 2, pp. 157-170, 1985.

[3] A. Nosier and J. Reddy, "On vibration and buckling of symmetric laminated plates according to shear deformation theories," *Acta mechanica,* vol. 94, no. 3-4, pp. 123-144, 1992.

[4] S. Hosseini-Hashemi, m. Fadaee, and S. R. Atashipour, "A new exact analytical approach for free vibration of Reissner–Mindlin functionally graded rectangular plates," *International Journal of Mechanical Sciences,* vol. 53, no. 1, pp. 11-22, 2011.

[5] S. H. Hashemi, S. R. Atashipour, and M. Fadaee, "An exact analytical approach for in-plane and out-of-plane free vibration analysis of thick laminated transversely isotropic plates," *Archive of Applied Mechanics,* vol. 82, no. 5, pp. 677-698, 2012.

[6] W. Cruz, N. Arzola, and O. Araque, "Modeling and experimental validation of the vibration in an unbalance multi-stage rotor," *Journal of Mechanical Engineering and Sciences,* vol. 13, no. 3, pp. 5703-5716, 2019.

[7] M. Merzuki, M. Rejab, M. Sani, B. Zhang, and M. Quanjin, "Experimental investigation of free vibration analysis on fibre metal composite laminates," *Journal of Mechanical Engineering and Sciences,* vol. 13, no. 4, pp. 5753-5763, 2019.

[8] H. Yaguchi, T. Mishina, and K. Ishikawa, "A new type of magnetic pump with coupled mechanical vibration and electromagnetic force," *Journal of Mechanical Engineering and Sciences,* vol. 13, no. 3, pp. 5212-5227, 2019.

[9] W. Chen and H. Ding, "On free vibration of a functionally graded piezoelectric rectangular plate," *Acta Mechanica,* vol. 153, no. 3-4, pp. 207-216, 2002.

[10] Z. Zhong and E. Shang, "Exact analysis of simply supported functionally graded piezothermoelectric plates," *Journal of Intelligent Material Systems and Structures,* vol. 16, no. 7-8, pp. 643-651, 2005.

[11] Z. Zhong and T. Yu, "Vibration of a simply supported functionally graded piezoelectric rectangular plate," *Smart materials and structures,* vol. 15, no. 5, p. 1404, 2006.

[12] h. s. Hosseini, h. akhavan, and M. Fadaee, "Exact closed-form free vibration analysis of moderately thick rectangular functionally graded plates with two bonded piezoelectric layers," 2011.

[13] K. Liew, Y. Xiang, and S. Kitipornchai, "Transverse vibration of thick rectangular plates—I. Comprehensive sets of boundary conditions," *Computers & structures*, vol. 49, no. 1, pp. 1-29, 1993.

[14] N. Bardell, R. Langley, and J. Dunsdon, "On the free in-plane vibration of isotropic rectangular plates," *Journal of Sound and Vibration*, vol. 191, no. 3, pp. 459-467, 1996.

[15] N. Farag and J. Pan, "Free and forced in-plane vibration of rectangular plates," *The Journal of the Acoustical Society of America*, vol. 103, no. 1, pp. 408-413, 1998.

[16] D. Gorman, "Free in-plane vibration analysis of rectangular plates by the method of superposition," *Journal of Sound and Vibration*, vol. 272, no. 3-5, pp. 831-851, 2004.

[17] D. Gorman, "Accurate analytical type solutions for the free in-plane vibration of clamped and simply supported rectangular plates," *Journal of sound and vibration*, vol. 276, no. 1-2, pp. 311-333, 2004.

[18] D. Gorman, "Exact solutions for the free in-plane vibration of rectangular plates with two opposite edges simply supported," *Journal of Sound and Vibration*, vol. 294, no. 1-2, pp. 131-161, 2006.

[19] S. H. Hashemi and A. Moradi, "Exact solutions for the in-plane vibrations of rectangular Mindlin plates using Helmholtz decomposition," *Acta mechanica*, vol. 215, no. 1-4, pp. 345-361, 2010.

[20] Y. Xing and B. Liu, "Exact solutions for the free in-plane vibrations of rectangular plates," *International Journal of Mechanical Sciences*, vol. 51, no. 3, pp. 246-255, 2009.

[21] L. Dozio, "In-plane free vibrations of single-layer and symmetrically laminated rectangular composite plates," *Composite Structures*, vol. 93, no. 7, pp. 1787-1800, 2011.

[22] E. Pan and P. Heyliger, "Free vibrations of simply supported and multilayered magneto-electro-elastic plates," *Journal of Sound and Vibration*, vol. 252, no. 3, pp. 429-442, 2002.

[23] G. R. Buchanan, "Layered versus multiphase magneto-electro-elastic composites," *Composites Part B: Engineering*, vol. 35, no. 5, pp. 413-420, 2004.

[24] M.-F. Liu and T.-P. Chang, "Closed form expression for the vibration problem of a transversely isotropic magneto-electro-elastic plate," *Journal of Applied Mechanics*, vol. 77, no. 2, 2010.

[25] Y. Li and J. Zhang, "Free vibration analysis of magnetoelectroelastic plate resting on a Pasternak foundation," *Smart materials and structures*, vol. 23, no. 2, p. 025002, 2013.

[26] L.-L. Ke, Y.-S. Wang, J. Yang, and S. Kitipornchai, "The size-dependent vibration of embedded magneto-electro-elastic cylindrical nanoshells," *Smart Materials and Structures*, vol. 23, no. 12, p. 125036, 2014.

[27] R. K. Bhangale and N. Ganesan, "Free vibration studies of simply supported non-homogeneous functionally graded magneto-electro-elastic finite cylindrical shells," *Journal of Sound and Vibration*, vol. 288, no. 1-2, pp. 412-422, 2005.

[28] G. Buchanan, "Free vibration of an infinite magneto-electro-elastic cylinder," *Journal of sound and vibration*, vol. 268, no. 2, pp. 413-426, 2003.

[29] C.-P. Wu and Y.-H. Tsai, "Dynamic responses of functionally graded magneto-electro-elastic shells with closed-circuit surface conditions using the method of multiple scales," *European Journal of Mechanics-A/Solids*, vol. 29, no. 2, pp. 166-181, 2010.

[30] C.-P. Wu and Y.-C. Lu, "A modified Pagano method for the 3D dynamic responses of functionally graded magneto-electro-elastic plates," *Composite structures*, vol. 90, no. 3, pp. 363-372, 2009.

[31] Y.-H. Tsai and C.-P. Wu, "Dynamic responses of functionally graded magneto-electro-elastic shells with open-circuit surface conditions," *International journal of engineering science*, vol. 46, no. 9, pp. 843-857, 2008.

[32] M. Hosseini, M. Mofidi, A. Jamalpoor, and M. S. Jahanshahi, "Nanoscale mass nanosensor based on the vibration analysis of embedded magneto-electro-elastic nanoplate made of FGMs via nonlocal Mindlin plate theory," *Microsystem Technologies*, vol. 24, no. 5, pp. 2295-2316, 2018.

[33] A. Shooshtari and R. Mantashloo, "Linear and Nonlinear Free Vibration of a Functionally Graded Magneto-electro-elastic Rectangular Plate Based on the Third Order Shear Deformation Theory," 2018.

[34] M. Karama, K. Afaq, and S. Mistou, "Mechanical behaviour of laminated composite beam by the new multi-layered laminated composite structures model with transverse shear stress continuity," *International Journal of solids and structures*, vol. 40, no. 6, pp. 1525-1546, 2003.

[35] A. S. Sayyad and Y. M. Ghugal, "Bending and free vibration analysis of thick isotropic plates by using exponential shear deformation theory," *Applied and Computational mechanics*, vol. 6, no. 1, 2012.

[36] S. Kharde, A. Mahale, K. Bhosale, and S. Thorat, "Flexural vibration of thick isotropic plates by using exponential shear deformation theory," *IJETAE*, vol. 3, no. 1, pp. 369-374, 2013.

[37] K. Khorshidi, T. Asgari, and A. Fallah, "Free vibrations analysis of functionally graded rectangular nano-plates based on nonlocal exponential shear deformation theory," *Mechanics of Advanced Composite Structures*, vol. 2, no. 2, pp. 79-93, 2015.

[38] K. Khorshidi and A. Fallah, "Buckling analysis of functionally graded rectangular nano-plate based on nonlocal exponential shear deformation theory," *International Journal of Mechanical Sciences*, vol. 113, pp. 94-104, 2016.

[39] k. Khorshidi, a. fallah, and a. siahpush, "Free vibrations analaysis of functionally graded composite rectangular nanoplate based on nonlocal exponential shear deformation theory in thermal environment," 2017.